Modeling and Simulation of Atomic Layer Deposition

Lado Filipovic

Institute for Microelectronics, Technische Universität Wien, Gußhausstraße 27-29/E360, 1040 Vienna, Austria
filipovic@iue.tuwien.ac.at

Abstract—**Two models for ALD of TiN and TiO$_2$ are incorporated in an in-house level set based topography simulator, ViennaTS. While the models are based on 1D surface kinetics, here they are extended to handle 2D and 3D geometries by applying single particle Monte Carlo ray tracing. The particle flux and sticking coefficients are used to calibrate the surface adsorption of precursors and ultimately to calculate the resulting surface velocity. The TiO$_2$ ALD model is based on the use of TTIP and H$_2$O precursors and includes all surface kinetics taking place during deposition. In contract, the model for the deposition of TiN is somewhat simplified by ignoring the purge steps which are introduced after surface exposure to either precursor. The simplified model is then applied to reproduce experimental results from plasma enhanced ALD process for TiN deposition from TDMAT and H$_2$-N$_2$ plasma precursors.**

Index Terms—**Atomic layer deposition, modeling and simulation, level set, TiN, TiO$_2$**

I. INTRODUCTION

TSMC has recently reported on vertically stacked lateral nanowire FETs where the high-k dielectric stack allows for a sub-1nm equivalent oxide thickness (EOT) and a sub-2nm physical thickness [1]. This was achieved using atomic layer deposition (ALD), the emergence of which was deemed essential to allow for the deposition of sub-2nm barrier layers [2]. ALD has been adopted aggressively at newer technology nodes and this trend is expected to continue well into future technology nodes at least until 2033, when a 0.5nm thin TiN barrier metal is foreseen to be used to limit copper (Cu) vacancy diffusion into the adjacent dielectric [3]. To ensure conformal deposition of thin TiN layers, alternatives to chemical vapor deposition (CVD) such as ALD are essential. In this manuscript, we describe two models for ALD and their implementation in the Level Set (LS) based feature-scale process and topography simulator ViennaTS [4].

ViennaTS is a Level Set framework which uses ray tracing and Monte Carlo methods to simulate the topography evolution of a surface after it is exposed to a given chemical reaction in a deposition/etching chamber. The simulator addresses the feature scale region of a wafer and for all models implemented thus far, the reactions on the surface were assumed to follow the Knudsen Law, meaning the diffusion length is smaller than the mean free path of the involved particles. Using ray tracing, the surface coverages for all involved particles

needs to be calculated, which directly influence the surface velocities. When simulating classical processes such as CVD the coverages are assumed to reach a steady state prior to applying a surface velocity. This cannot be assumed for ALD since the steady state will always be full coverage from a precursor. Therefore, in order to perform transient simulations of ALD, time discretization must be performed to track surface coverages during each step in the ALD process.

II. ATOMIC LAYER DEPOSITION

ALD is a cyclical process which proceeds with the sequential use of gas phase processes with two chemical precursors, as depicted in Fig. 1. In the first step, an atom or molecule A adsorbs on the surface while, during the second step, the chemical reaction between the adsorbed species and the gas atom or molecule B in the chamber results in the formation of one monolayer (ML) of a desired film AB. In the next cycle, species A adsorbs on the newly formed film AB in the first step, while in the subsequent step, species B once again reacts with the adsorbed A to form the second monolayer of film AB. This continues until the desired thickness or number of monolayers of AB is reached. In this manuscript, two models are addressed; the first one includes the simultaneous adsorption and desorption of precursors as well as pyrolytic and hyrolytic decomposition [5]. The second model is an alternative simplified implementation which ignores decomposition, thereby also avoiding the need to simulate the purge steps taking place after each gas phase during ALD [6].
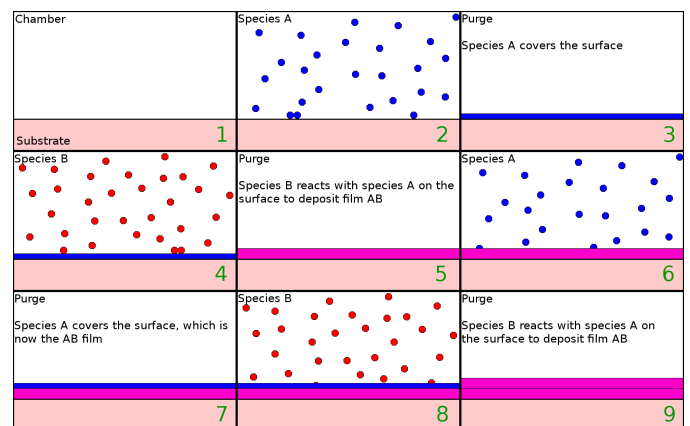

Fig. 1. ALD implemented with sequential use of gas phase processes with two chemical precursors (A and B) to form two monolayers of film AB.

III. ALD MODELS

Two models for ALD have been implemented in an in-house topography simulator ViennaTS. The advantage of the models' implementation therein is its integration with other simulation steps in a full CMOS fabrication sequence and the ability to use them to analyze the influence of several parameters on two-dimensional (2D) and three-dimensional (3D) geometries. In the models, the surface coverages of the precursors are tracked in time and converted to a surface velocity at each step.

A. TiO_2-ALD using TTIP and H_2O

A model for the deposition of titanium dioxide (TiO_2) using cycles of precursor titanium tetraisopropoxide (TTIP) and water (H_2O) has been presented by [5] and includes the adsorption and desorption of precursors as well as pyrolytic and hydrolytic decomposition. TiO_2 has several potential applications due to its mixed ionic-electronic conducting properties [7] and is currently implemented in the memristor [8]. The surface kinetics taking place during the TTIP and H_2O precursor stages are depicted in Fig. 2. The adsorption of species depends on the impinging rates (J_X) and sticking coefficient (S_X). The desorption processes include hydrolytic decomposition at a rate of $k_{hydrolysis}$ and in the case of TTIP, an additional pyrolytic decomposition process takes place, with a rate of $k_{pyrolysis}$. In the above discussion X refers to $TTIP$ or H_2O, depending on which step in the cycle is being observed. During the purge steps, desorption, hydrolysis, and pyrolysis continues to take place [5].
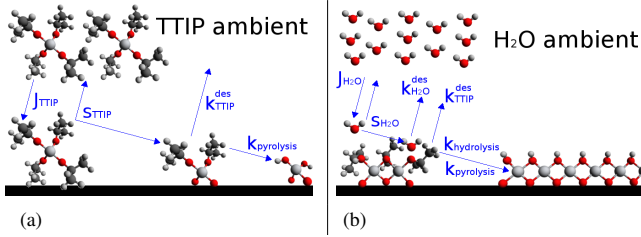

Fig. 2. Schematic representation of the surface kinetics during (a) the TTIP step and the (b) H_2O step.

The equations which describe the TTIP and H_2O coverages θ_X during their respective steps in the ALD cycle are given in equations (1) and (2), respectively. All reactions k_X are expressed by an Arrhenius law and for the exact parameter values which correspond to measurements, refer to [5]. The following equations shows the calculation of the change in TTIP and H_2O coverage with time during each respective cycle; θ_X^0 represent the total available surface coverage sites.

TTIP step:

$$\begin{aligned}
\frac{d\theta_{TTIP}}{dt} =\ & J_{TTIP}S_{TTIP}\left(1 - \frac{\theta_{TTIP}}{\theta_{TTIP}^0}\right) - k_{TTIP}^{des}\theta_{TTIP} \\
& - k_{hydrol}\theta_{TTIP}\theta_{H_2O} - k_{pyrol}\theta_{TTIP}^2
\end{aligned} \quad (1)$$

H_2O step:

$$\begin{aligned}
\frac{d\theta_{H_2O}}{dt} =\ & J_{H_2O}S_{H_2O}\left(1 - \frac{\theta_{H_2O}}{\theta_{H_2O}^0}\right) - k_{H_2O}^{des}\theta_{H_2O} \\
& - k_{hydrol}\theta_{TTIP}\theta_{H_2O}
\end{aligned} \quad (2)$$

Since the decomposition processes also take place during the purge steps, the surface coverages can change during this time. Also, surface deposition takes place only when both TTIP and H_2O are both covering a section of the surface and as the film is deposited, the TTIP coverage is reduced, as shown in the single-cycle simulation in Fig. 3. The growth rate applied in the topography simulator depends on the thickness of a single molecular layer of TiO_2 (ML_{TiO}) and follows

$$Rate = ML_{TiO}\ (\theta_{TTIP}\theta_{H_2O}). \quad (3)$$
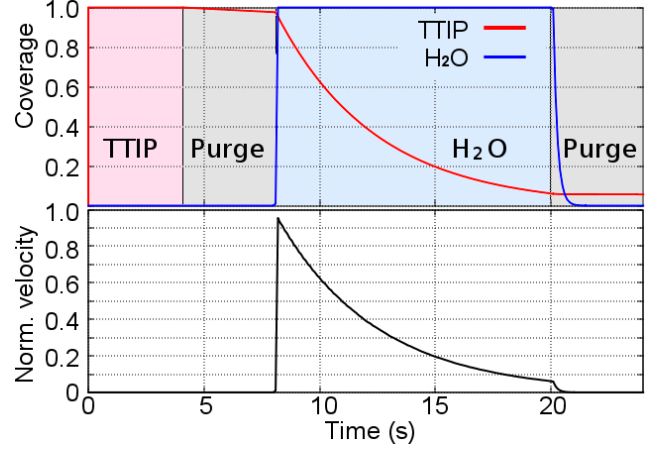

Fig. 3. Single cycle of the TiO_2 ALD process showing the coverages of TTIP and H_2O and the resulting surface velocity.

B. TiN-ALD using TDMAT and NH_3

In this section the ALD model for TiN deposition is described and a sample simulation is performed on a trench geometry. The purge steps are ignored since their influence on the surface coverages are minimal. The core of the model is the one-dimensional (1D) surface kinetics description of TiN-ALD using tetrakis(dimethylamido)titanium (TDMAT) and ammonia (NH_3) given in [6]. Since the base model is 1D, we improve on the implementation by extending it to reflect the influence of the sticking coefficient (s) of an atom or molecule on the surface coverage using Monte Carlo (MC) ray tracing in a LS framework. In this work we enable ALD simulation of a generic film *AB* from a cycle which includes adsorption of species *A* followed by species *B*. The universality of the model is demonstrated here by using it to simulate TiN plasma enhanced ALD (PE-ALD) by calibrating four adsorption parameters.

The TDMAT molecule, adsorbed on top of the substrate - or on the TiN film - in the first step of the ALD cycle reacts with the NH_3 from the second step, resulting in the deposition of TiN. Furthermore, during the second step, NH_3 can be adsorbed on the TiN, which is either the TiN formed by the reaction or the TiN which becomes an outer surface again after the adsorbed TDMAT has been removed by reaction with NH_3, shown in Fig. 4. These NH_3 molecules can serve to form TiN with the TDMAT from the first step in the next cycle. Therefore, it is possible that more than one monolayer (ML)

of TiN is deposited in a single cycle [6]. In the simulation, this means that different coverages ($\theta_{X/Y}$) must be tracked consistently, as follows:

TDMAT step:

$$
\begin{aligned}
\frac{d\theta_{TDMAT/NH_3}}{dt} =\ & C_{TDMAT/NH_3} \\
& \times \left(\theta^{NH_3} - \theta_{TDMAT/NH_3}\right)^{n_{TDMAT}} \\
\frac{d\theta_{TDMAT/TiN}}{dt} =\ & C_{TDMAT/TiN} \\
& \times \left(\theta^{TiN} + \theta_{TDMAT/NH_3} - \theta_{TDMAT/TiN}\right)^{n_{TDMAT}}
\end{aligned}
\tag{4}
$$

NH$_3$ step:

$$
\begin{aligned}
\frac{d\theta_{NH_3/TDMAT}}{dt} =\ & C_{NH_3/TDMAT} \\
& \times \left(\theta^{NH_3} - \theta_{NH_3/TDMAT}\right)^{n_{NH_3}} \\
\frac{d\theta_{NH_3/TiN}}{dt} =\ & C_{NH_3/TiN} \\
& \times \left(\theta^{TiN} + \theta_{NH_3/TDMAT} - \theta_{NH_3/TiN}\right)^{n_{NH_3}}
\end{aligned}
\tag{5}
$$

In equations (4) and (5) above, $\theta_{X/Y}$ represents the adsorption coverage of species X on the film in the vicinity of adsorbed species Y and $\theta_{X/TiN}$ is the adsorption coverage of molecule X on the exposed TiN surface; θ^X is the coverage of species X at the end of the previous cycle; $C_{X/Y}$ is the adsorption constant for the adsorption of X onto Y; n_X is the adsorption order of the X molecule. Species X and Y can correspond to either the TDMAT or NH$_3$ molecule or, in a universal manner, to the molecule or atom of any reacting species A or B.
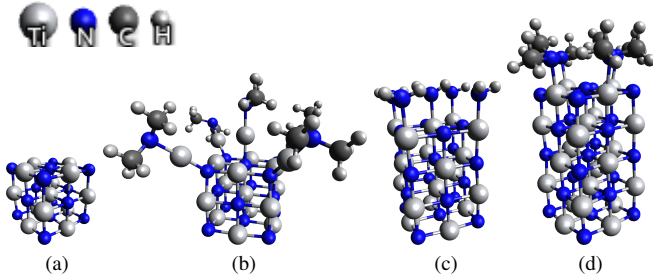

Fig. 4. TiN-ALD cycle with (a) the TiN unit cell, (b) after a single TDMAT step, (c) after a subsequent NH$_3$ step, and (d) after a 2$^{\text{nd}}$ TDMAT step.

1) Surface Velocity Calculation: While solving the coverage equations during CVD or plasma etching simulations, it is appropriate to assume that surface reactions are very fast, reaching a steady state before any deposition and etching takes place. However, this is not true of ALD, where coverages must be solved in time. Also, the set of coverage equations for both ALD steps, relating to the adsorption of molecules on the exposed TiN surface cannot be solved analytically and therefore approximations are used in the simulation. In order to account for this, time discretization for the calculation of surface coverages is introduced in ViennaTS; this requires a calibration between the time step used for the coverage calculation and the time step used for the LS surface evolution. Time discretization is implemented dynamically and the size of each step depends on the maximum allowed error, as set in the parameters file during runtime.

Another concern with this ALD process is that when TD-MAT reacts with adsorbed NH$_3$ to form TiN, there is a volume reduction taking place. The NH$_3$ molecule is much larger than a TiN molecule, when in the gas phase. Although the adsorbed reactants are not in the same chemical states as those in the gas phase, the ratio of the difference in molecular size is considered to evaluate a parameter m_X which represents the volume reduction and is used for the calculation of the maximum growth rate [6]. In the case of the TiN-ALD process, $m_{NH_3} = 4$ and $m_{TDMAT} = 1$. The TiN film thickness increase in a single cycle, in terms of ML/cycle, is therefore calculated using

$$
Rate\,(ML/cycle) = \frac{\theta_{TDMAT/NH_3}}{m_{NH_3}} + \frac{\theta_{NH_3/TDMAT}}{m_{TDMAT}}, \quad (6)
$$

where m_X refers to the reduction ratio of an occupied surface area when an adsorbed species X reacts with a gas molecule Y to form TiN. To determine the surface velocity, we note the thickness of a ML of TiN $ML_{TiN} = 0.4$ nm and that deposition occurs only when there is a change in coverage $\Delta\theta_{X/Y}$ during a time step Δt. The surface velocity is therefore determined by the change in the coverage per time step and is calculated using

$$
V = \frac{ML_{TiN}}{\Delta t}\left(\frac{\Delta\theta_{TDMAT/NH_3}}{m_{NH_3}} + \frac{\Delta\theta_{NH_3/TDMAT}}{m_{TDMAT}}\right). \quad (7)
$$

Note that the thickness per cycle $Rate(ML/cycle)$ calculated from equation (6) is obtained by integrating the surface velocity over the time of one full cycle. In Fig. 5 we plot the relationship between the surface velocity and respective coverages when using 1.5s and 3s step sizes for the TDMAT and NH$_3$ steps, respectively. It is evident that a surface velocity is only applied when the coverages are changing.
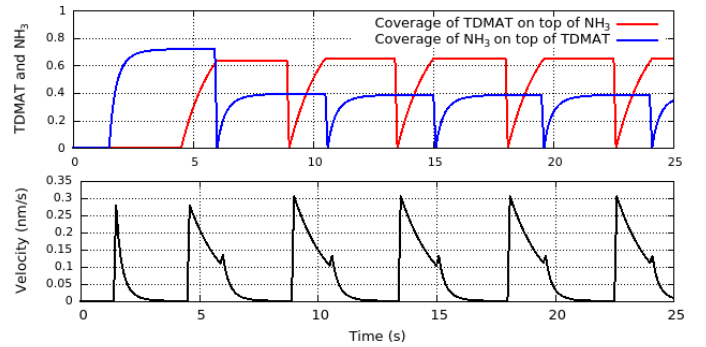

Fig. 5. Coverages (top) and the resulting surface velocity (bottom) when the TDMAT and NH$_3$ steps are set to 1.5s and 3s, respectively.

2) Model Extensions: In order to extend the above model to 2D and 3D geometries we introduce MC ray tracing, with a flux (J) and sticking coefficient (s) assigned to each involved precursor. This allows to further generalize the model to any precipitate and desired film. The effects of the surface flux are included by setting the adsorption constant relative to the distribution of the incoming MC particles using

$$
C_{X/Y} = J_X \cdot s_X. \tag{8}
$$

Based on the experimental results from [6] we find that s for TDMAT and NH$_3$ is in the order of approximately 10^{-5}, suggesting a highly conformal deposition. This means that the flux will see only a 13% drop at the bottom of a 3D cylindrical hole with aspect ratio (AR) of 100, when compared to the flux at the wafer top. However, this is not the case for all ALD processes, described in [9], where it is shown that, depending on the ALD precursors, s can vary by several orders of magnitude. In Fig. 6 we show a sample simulation on a trench with aspect ratio 2.5 and sticking coefficients $s_1 = 0.1$ and $s_2 = 0.2$, while varying the ALD cycle step times and the number of cycles. As an example, these values of s are in the range observed for Al(CH$_3$)$_3$ and O plasma precursors for the deposition of Al$_2$O$_3$ [9].
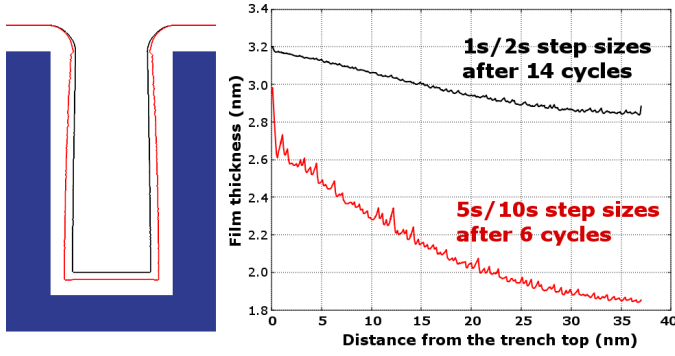

Fig. 6. The deposited film surface after a simulation of several cycles for a generic ALD model on a trench geometry with 2.5 AR using sticking probabilities 0.1 and 0.2 for species A and B, respectively.

C. Plasma Enhanced ALD

The TiN-ALD model described in the previous section and implemented in a level set framework was further applied to a low-temperature PE-ALD process to simulate the deposition of a thin TiN film using TDMAT and H$_2$-N$_2$ plasma as precursors using experiments from Caubet et al. [10]. The TiN film growth takes place almost exclusively during the plasma step with H$_2$-N$_2$ and the deposition rate is much faster than observed in the classical ALD. According to [10] no re-emission takes place; therefore, calculating the coverages of TDMAT (9) and H$_2$-N$_2$ (10) simplifies to:

TDMAT step:

$$
\begin{aligned}
\frac{d\theta_{TDMAT/H-N}}{dt} = \ & C_{TDMAT/H-N} \\
& \times \left(\theta^{H/N} - \theta_{TDMAT/H-N} \right)^{n_{TDMAT}}
\end{aligned}
\tag{9}
$$

H$_2$-N$_2$ step:

$$
\begin{aligned}
\frac{d\theta_{H-N/TDMAT}}{dt} = \ & C_{H-N/TDMAT} \\
& \times \left(\theta^{TDMAT} - \theta_{H-N/TDMAT} \right)^{n_{H-N}}
\end{aligned}
\tag{10}
$$

Since the deposition of TiN takes place exclusively during the H$_2$-N$_2$ plasma step, the TDMAT serves to prepare the surface with the appropriate coverages for the subsequent plasma deposition step. Furthermore, since N reacts directly with exposed Ti and not with NH$_3$, no volume reduction needs consideration and m_X can be ignored. The surface rate is then

$$
Rate\,(ML/cycle) = \theta_{H-N/TDMAT}
\tag{11}
$$

and the resulting surface velocity is calculated using

$$
V = \frac{ML_{TiN}}{\Delta t} \left(\Delta\theta_{H-N/TDMAT} \right).
\tag{12}
$$

Using the above equations, the model the experimental results for a PE-ALD process described in [10] were replicated by adjusting the adsorption parameters, given on the right of Fig. 7, where the comparison between the simulated and experimental coverage is shown. This step determines how much TDMAT is adsorbed at the surface to prepare for the subsequent bonding with N atoms during the plasma step. Since the coverage during the plasma step is very fast, the TDMAT is the critical parameter for fast deposition.
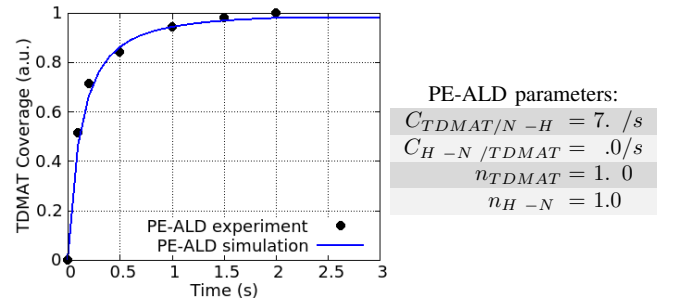

Fig. 7. Comparison between the experimental measurements from [10] and the PE-ALD model, with the adsorption parameters shown on the right.

IV. Conclusion

Two models for atomic layer deposition were presented and incorporated in a level set based topography simulator, ViennaTS. The models are for the deposition of TiO$_2$ and TiN from different precursors and are both based on one-dimensional surface kinetics. However, they have been extended to 2D and 3D geometries by introducing MC ray tracing and the influence of particle flux and sticking coefficients on the surface adsorption and resulting deposition velocity. The ALD-TiO$_2$ model is quite complex and includes adsorption and desorption of precursors as well as pyrolytic and hydrolytic decomposition. An alternative simplified universal model for TiN-ALD was also introduced in the level set environment. With these models we have reproduced experimental results from an ALD-TiO$_2$ and ALD-TiN processes as well as a PE-ALD process from TDMAT and H$_2$-N$_2$ plasma precursors.

References

[1] M. van Dal et al. in *IEEE IEDM*, 2018, 492–495.
[2] "ITRS," IRC, Tech. Rep., 2013.
[3] "IRDS," IEEE, Tech. Rep., 2017.
[4] *ViennaTS User Guide*, Vienna, Austria: TU Wien, 2019.
[5] M. Reinke et al., *J. Phys. Chem. C*, 119(50), 27 965–27 971, 2015.
[6] J.-W. Lim et al., *J. Appl. Phys.*, 87(9), 4632–4634, 2000.
[7] H. Lim et al., *Nanotechnology*, 24(38), 384005(8pp), 2013.
[8] X. Yan et al., *Adv. Funct. Mater.*, 28(1), 1705320(9), 2018.
[9] H. Knoops et al., *J. Electrochem. Soc.*, 157(12), G241–G249, 2010.
[10] P. Caubet et al., *J. Electrochem. Soc.*, 155(8), H625–H632, 2008.